ceptor-chromatin interaction or abnormal androgen-mediated transcription (*15*), it cannot be claimed that retention of the H-Y$^+$ cellular phenotype depends on testosterone or on any male characteristic that is secondary to any action of testosterone.

These findings are consistent with our hypothesis that H-Y is the primary determinant of male gonadal sex in XY-male species. This conclusion has practical as well as theoretical implications, for it bears on the ultimate value of H-Y typing as a diagnostic measure in the appraisal of cases of abnormal sexual development in man.

GLORIA C. KOO, STEPHEN S. WACHTEL
Memorial Sloan-Kettering Cancer Center, New York 10021
PAUL SAENGER, MARIA I. NEW
Department of Pediatrics, New York Hospital–Cornell Medical Center, New York 10021
HARVEY DOSIK
Department of Hematology, Jewish Hospital and Medical Center of Brooklyn, Brooklyn, New York 11238
ANTHONY P. AMAROSE
ELIZABETH DORUS
Department of Obstetrics and Gynecology, and *Department of Psychiatry, University of Chicago, Chicago, Illinois 60637*
VALERIO VENTRUTO
Ospedale Cardarelli, Naples, Italy

References and Notes

1. S. Ohno, *Cell* **7**, 315 (1976).
2. W. J. Meyer, B. R. Migeon, C. J. Migeon, *Proc. Natl. Acad. Sci. U.S.A.* **72**, 1469 (1975).
3. J. M. Morris, *Am. J. Obstet. Gynecol.* **65**, 1192 (1953).
4. A. L. Southren, G. G. Gordon, S. Tochimoto, *J. Clin. Endocrinol.* **28**, 1105 (1968).
5. R. R. Tremblay, T. P. Foley, Jr., P. Corvol, I. J. Park, A. Kowarski, R. M. Blizzard, H. W. Jones, Jr., C. J. Migeon, *Acta Endocrinol.* **70**, 331 (1972).
6. A. L. Strickland and F. S. French, *J. Clin. Endocrinol.* **29**, 1284 (1969).
7. J. D. Wilson and J. L. Goldstein, *Birth Defects, Orig. Artic. Ser.* **11**, 1 (1975).
8. E. J. Eichwald and C. R. Silmser, *Transplant. Bull.* **2**, 154 (1955).
9. S. S. Wachtel, *Immunol. Rev.* **33**, 33 (1977); R. P. Erickson, *Nature (London)* **265**, 59 (1977).
10. S. S. Wachtel, E. H. Goldberg, E. E. Zuckerman, E. A. Boyse, *Nature (London)* **244**, 102 (1973).
11. S. S. Wachtel, G. C. Koo, E. A. Boyse, *ibid.* **254**, 270 (1975).
12. S. S. Wachtel, S. Ohno, G. C. Koo, E. A. Boyse, *ibid.* **257**, 235 (1975).
13. D. Bennett, B. J. Mathieson, M. Scheid, K. Yanagisawa, E. A. Boyse, S. S. Wachtel, B. M. Cattanach, *ibid.* **265**, 255 (1977).
14. D. Bennett, E. A. Boyse, M. F. Lyon, B. J. Mathieson, M. Scheid, K. Yanagisawa, *ibid.* **257**, 236 (1975).
15. J. A. Amrhein, W. J. Meyer, III, H. W. Jones, Jr., C. J. Migeon, *Proc. Natl. Acad. Sci. U.S.A.* **73**, 891 (1976).
16. S. Korth-Schutz, L. S. Levine, M. I. New, *J. Clin. Endocrinol.* **42**, 117 (1976).
17. I. Ito and R. Horton, *J. Clin. Invest.* **50**, 1621 (1971).
18. Supported by NIH grants CA-08748, AI-11982, HD-10065, HD-00171, GM-00984, HD-07110, CP-43251, and contract GCRC,RR47, by New York State Health Research Council grant 272, and by Rockefeller Foundation grant RF-74043.

22 November 1976

Spinal Neurons Project to the Dorsal Column Nuclei of Rhesus Monkeys

Abstract. *Cells of origin of ascending nonprimary afferents to the dorsal column nuclei of rhesus monkeys have been identified in the spinal cord by the retrograde transport of horseradish peroxidase. These neurons are mainly located in lamina IV and medially in more ventral laminae of the dorsal horn on the side ipsilateral to the medullary injection. Large neurons in the ventral horn ("spinal border cells") also appear to project to the ipsilateral dorsal medulla. The dorsal column nuclei of a primate thus are the recipient not only of ascending dorsal root fibers but also of a more complexly integrated spinal input.*

Traditional concepts concerning the organization and function of ascending sensory systems in the mammalian spinal cord are founded upon a dichotomy between the anterolateral and the dorsal column–medial lemniscal systems. The anterolateral ascending system comprises spinothalamic fibers which, in primates, originate mainly from neurons in the dorsal horn (*1*), ascend in the contralateral anterolateral funiculus of the spinal cord, and terminate in several thalamic nuclei (*2*). In the dorsal columns (or dorsal funiculi) ascend uncrossed fibers which originate from dorsal root ganglion cells and terminate in the dorsal column nuclei (DCN, including gracile and cuneate) in the caudal medulla oblongata. Fibers from cells in these nuclei cross, form the medial lemniscus, and also terminate in the thalamus (*2*). Transmission of different sensory modalities is usually attributed to these two major pathways, although some overlap seems to exist in the role that these two systems play in the mediation of somatic sensibility (*3*).

Recent anatomical and electrophysiological data have shown that the dorsal column nuclei of higher mammals are the target not only of dorsal root afferents, but also of fibers arising from the spinal gray matter and ascending in the dorsal and dorsolateral funiculi (*4*). In the present study, cells of origin of these ascending fibers have been visualized in the monkey by means of the retrograde transport of horseradish peroxidase (HRP) (*5*). Like spinothalamic cells in the same species, spino-DCN cells are mainly located in the dorsal horn; therefore, the spinothalamic tract and the dorsal column nuclei–medial lemniscus pathway convey ascending information relayed by cells which are accessible to activation by similar peripheral input.

In six adult rhesus monkeys, 30 percent HRP (Sigma type VI or Boeringher) was injected either unilaterally or bilaterally into the dorsal medulla. All animals were anesthetized with Nembutal (40 mg/kg, intraperitoneally) and were held in the frame of a stereotaxic apparatus. After removal of a small portion of the occipital bone and incision of the dura mater, part of the posterior cerebellum was aspirated. By this approach the dorsal aspect of the DCN throughout the rostrocaudal extent was exposed. Single or multiple injections totaling 0.05 to 0.5 μl per side were made with a CR700-20 Hamilton syringe fitted with a 26S gauge needle (outer diameter 0.5 mm, inner diameter 0.37 mm). After 48 to 72 hours all animals were perfused with 0.9 percent saline, followed by a double aldehyde mixture (0.5 percent paraformaldehyde and 2.5 percent glutaraldehyde in 0.1*M* phosphate buffer at *p*H 7.2). Immediately after perfusion the brain and spinal cord were removed and washed for at least 24 hours in 0.1*M* phosphate buffer at *p*H 7.2 to which 30 percent sucrose was added. Serial frozen 40-μm sections through the medulla and spinal cord were incubated for 30 minutes at room temperature in a 0.05 percent solution of 3,3′-diaminobenzidine-tetrahydrochloride in tris-HCl buffer (*p*H 7.6) to which freshly prepared 1 percent hydrogen peroxide was added (*6*). All sections were screened under dark- or bright-field illumination, and the locations of labeled cells were plotted on tracing paper with an electronic pantograph. The injection sites were reconstructed from serial transverse sections through the medulla with the aid of an overhead projector and of microscopic observation.

The extent of the HRP infiltration into the dorsal medulla and the number of labeled neurons in the spinal cord varied according to the total volume injected. In four cases in which the focus of the HRP infiltration was within the boundaries of the DCN, the majority of the labeled neurons were in the dorsal horn of both sides (after bilateral injections) or of the side ipsilateral to the injected medulla (after unilateral injection).

The results in one case with a unilateral injection are shown in Fig. 1. On the side ipsilateral to the injected medulla labeled cells in the upper three cervical segments were concentrated in the medial part of the dorsal horn and in the intermediate zone. Throughout the brachial and lum-

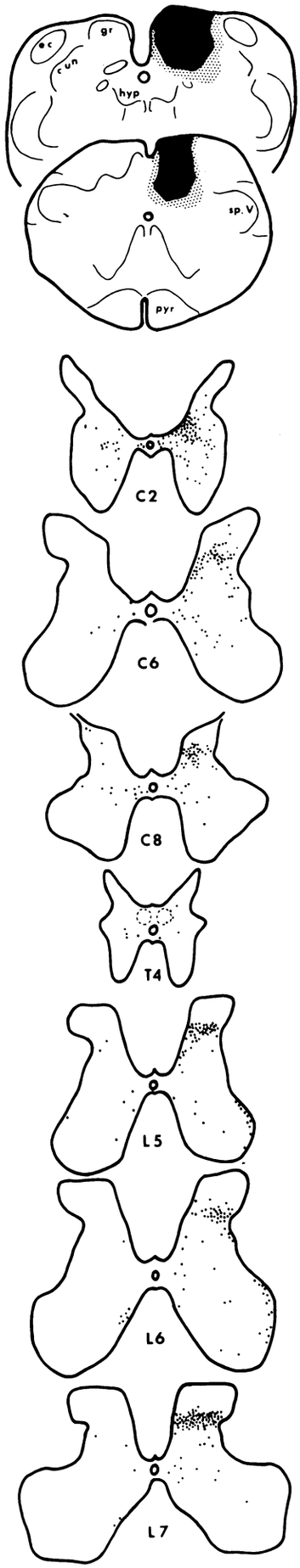

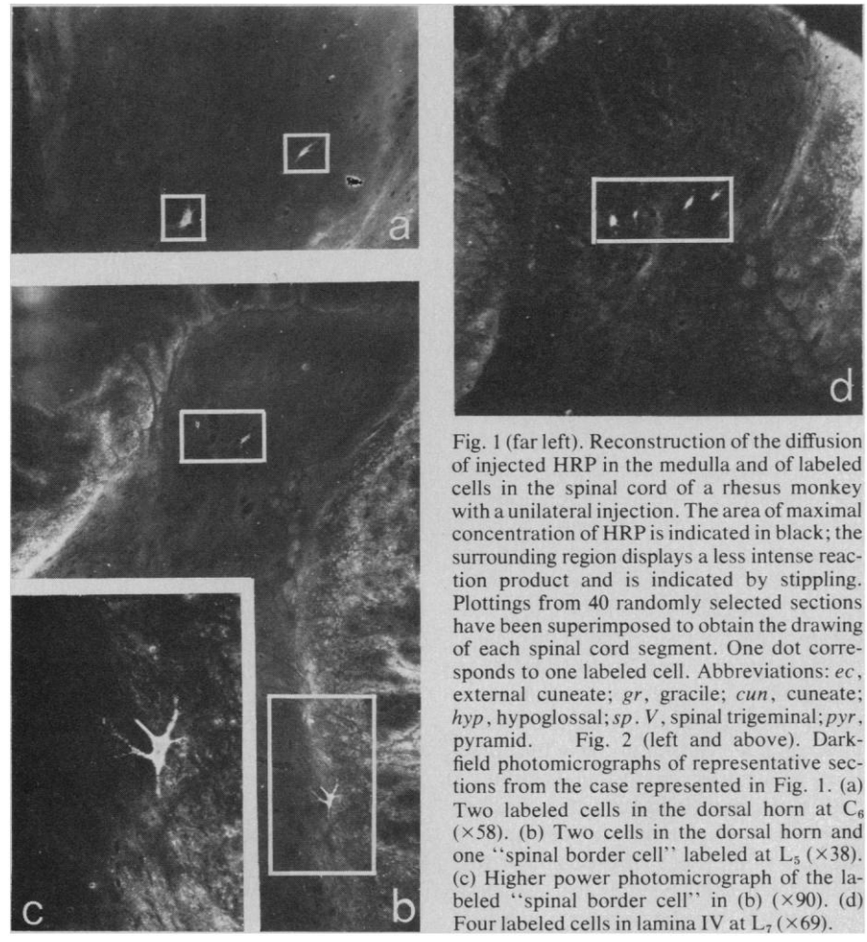

Fig. 1 (far left). Reconstruction of the diffusion of injected HRP in the medulla and of labeled cells in the spinal cord of a rhesus monkey with a unilateral injection. The area of maximal concentration of HRP is indicated in black; the surrounding region displays a less intense reaction product and is indicated by stippling. Plottings from 40 randomly selected sections have been superimposed to obtain the drawing of each spinal cord segment. One dot corresponds to one labeled cell. Abbreviations: *ec*, external cuneate; *gr*, gracile; *cun*, cuneate; *hyp*, hypoglossal; *sp. V*, spinal trigeminal; *pyr*, pyramid. Fig. 2 (left and above). Darkfield photomicrographs of representative sections from the case represented in Fig. 1. (a) Two labeled cells in the dorsal horn at C_6 (×58). (b) Two cells in the dorsal horn and one "spinal border cell" labeled at L_5 (×38). (c) Higher power photomicrograph of the labeled "spinal border cell" in (b) (×90). (d) Four labeled cells in lamina IV at L_7 (×69).

bosacral cord most labeled neurons were found in a region corresponding to lamina IV of the feline spinal cord (*7*) and medially in more ventral laminae of the dorsal horn (Fig. 2, a and d). Labeled cell bodies in the dorsal horn displayed various morphological types (multipolar, round, elongated, and so forth) and their largest diameter ranged from 18 to 50 μm. Relatively few labeled cells were distributed within the thoracic cord below T1. Large labeled neurons (up to 65 μm) were also labeled in the ventral horn of the lumbar cord ipsilateral to the injected side, especially in L4, L5 and L6 (Fig. 2, b and c). HRP-positive neurons in the ventral horn at these levels appear to be identifiable as "spinal border cells" (*8*). On the side of the spinal cord contralateral to the injection fewer labeled cells were present than ipsilaterally, and were scattered in the intermediate zone and dorsal horn. The results in the other three cases with HRP injections largely confined within the boundaries of the DCN were comparable to those shown in Fig. 1. In each case the number of labeled cells in the brachial and lumbosacral cord appeared to reflect the more or less complete infiltration of either the cuneate or the gracile nucleus.

In two cases, the injected HRP infiltrated the DCN but also diffused into several adjacent nuclear structures and fiber tracts. These included the dorsal motor nucleus of the vagus, hypoglossal nucleus, nucleus intercalatus, solitary nucleus and tract, nucleus Z, external cuneate nucleus, and parts of the medullary tegmentum and of the spinal trigeminal complex (pars caudalis). Involvement of these more ventrally and laterally located medullary regions resulted in profuse labeling throughout the dorsal horn and intermediate zone of the upper cervical segments. At more caudal levels, labeled cells were mainly distributed as shown in Fig. 1, although they were also present in the marginal zone (lamina I) and were more numerous in the intermediate zone than in cases with more restricted injections.

From comparison of the results in all of the present cases it appears that spinal cells of origin of ascending fibers to the DCN are located mainly in lamina IV and in the medial portion of the ventral laminae of the dorsal horn. These results are in good agreement with recent observations on the feline spinal cord (*9*). In addition, at least some of the "spinal border cells" in the monkey project to the ipsila-

teral dorsal medulla, most likely to the DCN. This finding cannot be ascribed to diffusion of injected HRP into the ventral spinocerebellar tract, which takes origin from such cells but is mainly crossed and runs along the ventrolateral margin of the medulla (*10*).

Cells in lamina IV, in which the majority of spino-DCN neurons appear to be located, are responsive to a wide range of mechanical stimuli applied to glabrous and hairy skin (*11*), and are modulated by activity in descending supraspinal pathways (*12*). Thus, besides receiving direct afferents via dorsal root fibers, the DCN are the relay of an ascending input which has undergone complex integration at segmental levels. Spinothalamic cells activated by hair movements and by low threshold mechanical deformation of the skin (*13*) and cells of origin of spinocervical tract (*14*) are also found in this region of the primate dorsal horn. Whether at least some of the fibers in the spinocervical, spinothalamic, and spino-DCN tracts have common cells of origin in the dorsal horn is a matter for further anatomical and electrophysiological investigation. However, it is legitimate to postulate, on the basis of the present observations, that these three pathways in the rhesus monkey may share some common functional properties.

ALDO RUSTIONI
Departments of Anatomy and
Physiology, University of
North Carolina, Chapel Hill 27514

References and Notes

1. D. L. Trevino, J. D. Coulter, W. D. Willis, *J. Neurophysiol.* **36**, 750 (1973); D. L. Trevino and E. Carstens, *Brain Res.* **98**, 177 (1975).
2. J. J. G. Boivie and E. R. Perl, in *MTP International Review of Science*, Neurophysiology Series, C. C. Hunt, Ed. (University Park Press, Baltimore, 1975), vol. 3, pp. 303–411; J. L. DeVito and D. M. Simmons, *Exp. Neurol.* **51**, 347 (1976).
3. C. J. Vierck, D. H. Hamilton, J. I. Thornby, *Exp. Brain Res.* **13**, 140 (1971); J. Semmes, in *Handbook of Sensory Physiology*, A. Iggo, Ed. (Springer-Verlag, New York, 1973), vol. 2, pp. 719–742; D. Angaut-Petit, *Exp. Brain Res.* **22**, 471 (1975); W. Noordenboos and P. D. Wall, *Pain* **2**, 185 (1976).
4. A. M. Dart and G. Gordon, *Brain Res.* **58**, 61 (1973); A. Rustioni, *ibid.* **51**, 81 (1973); D. Angaut-Petit, *Exp. Brain Res.* **23**, 1 (1975); D. E. Nijensohn and F. W. L. Kerr, *J. Comp. Neurol.* **161**, 459 (1975).
5. K. Kristensson and Y. Olson, *Brain Res.* **29**, 363 (1971); J. H. LaVail and M. M. LaVail, *Science* **176**, 1416 (1972).
6. R. C. Graham and M. J. Karnovsky, *J. Exp. Med.* **14**, 291 (1966).
7. B. Rexed, *J. Comp. Neurol.* **96**, 415 (1952); **100**, 297 (1954).
8. S. Cooper and C. W. Sherrington, *Brain* **63**, 123 (1940).
9. A. Rustioni and A. B. Kaufman, *Exp. Brain Res.* **27**, 1 (1977).
10. A. Brodal, *Neurological Anatomy* (Oxford Univ. Press, New York, 1969), pp. 274–275; E. Jankowska and S. Lindström, *Brain Res.* **20**, 323 (1970); R. Burke, A. Lundberg, F. Weight, *Exp. Brain Res.* **12**, 283 (1971).
11. I. H. Wagman and D. D. Price, *J. Neurophysiol.* **32**, 803 (1969); D. D. Price and D. J. Mayer, *Brain Res.* **79**, 321 (1974).
12. P. D. Wall, *J. Physiol.* **188**, 403 (1967); E. E. Fetz, *J. Neurophysiol.* **31**, 69 (1968); A. G. Brown, in *Handbook of Sensory Physiology*, A. Iggo, Ed. (Springer-Verlag, New York, 1973), vol. 2, pp. 315–338; J. D. Coulter, R. A. Maunz, W. D. Willis, *Brain Res.* **65**, 351 (1974).
13. W. D. Willis, D. L. Trevino, J. D. Coulter, R. A. Maunz, *J. Neurophysiol.* **37**, 358 (1974); D. D. Price and D. J. Mayer, *Pain* **1**, 59 (1975).
14. R. N. Bryan, J. D. Coulter, W. D. Willis, *Exp. Neurol.* **42**, 574 (1974).
15. Supported by NIH grant NS12440. I thank Dr. M. Kuno for his suggestions and comments pertaining to the manuscript and A. B. Kaufman for technical assistance.

13 December 1976

Degradation and Detoxification of Canavanine by a Specialized Seed Predator

Abstract. *Larvae of the bruchid beetle* Caryedes brasiliensis *feed exclusively on seeds of the Neotropical legume* Dioclea megacarpa, *which contains 13 percent* L-*canavanine by dry weight.* L-*Canavanine, a nonprotein amino acid analog of* L-*arginine, exhibits potent insecticidal properties. Most of the seed nitrogen is sequestered in canavanine, and bruchid beetle larvae do not simply excrete this toxic compound. Instead, these larvae possess extraordinarily high urease activity, which facilitates the conversion of canavanine to ammonia through urea. In this way, canavanine is effectively detoxified and a supply of nitrogen for fixation into organic linkage is ensured.*

Larvae of the bruchid beetle *Caryedes brasiliensis* feed exclusively on the seeds of the Neotropical legume *Dioclea megacarpa* (*1*), which contains 13 percent L-canavanine by dry weight (*2*). L-Canavanine is a toxic structural analog of L-arginine whose potent insecticidal properties have been thoroughly established in studies with various insects (*3*). We recently reported that larvae of *C. brasiliensis* possess an arginyl-tRNA synthetase that discriminates between arginine and canavanine so that canavanine-containing proteins are not synthesized (*4*). As a result, these bruchid beetle larvae avoid the most deleterious consequence of canavanine consumption (*5*). This bruchid beetle may simply excrete canavanine, sacrificing this abundant source of seed nitrogen, or it may have developed the ability to utilize this toxic substance. We report here the first demonstration, to our knowledge, of an insect that converts a poisonous plant substance to a foodstuff, providing nitrogen for primary metabolic pathways.

Analysis of *D. megacarpa* seeds infested with *C. brasiliensis* revealed that developing larvae ingest appreciable canavanine (Table 1). Undigested canavanine occurred in the frass, but nearly 60 percent of the seed canavanine was metabolized (Table 1) (*6*). Enzymatic assay of a homogenate of the larvae revealed the presence of appreciable arginase (*7*), the enzyme that mediates the cleavage of L-arginine or L-canavanine to urea and L-ornithine or L-canaline, re-

Table 1. Metabolism of L-canavanine by larvae of the bruchid beetle *C. brasiliensis* that developed in the seed of *D. megacarpa*. The dry weight of individual intact seeds was calculated by regression analysis of intact seed dry weight on testa dry weight ($y = -7.08 + 5.85x$). Uneaten seed and insect frass were collected from each infested seed, ground by hand, and dried to constant weight at 70°C. Canavanine was extracted by mechanical stirring of the dried samples with 100 volumes of 50 percent aqueous ethanol containing 0.1*N* HCl at 10°C for 18 hours. After the resulting slurry was clarified by centrifugation at 23,000*g* for 15 minutes, the pellet was reextracted with 50 volumes of the solvent for 6 hours at 10°C. Canavanine content was determined by the colorimetric assay method described by Rosenthal (*13*). The term seed denotes cotyledons plus embryonic tissues minus testa.

Dry weight (g)		Canavanine content (μmole)				Canavanine metabolized (μmole)	Ingested seed canavanine metabolized (%)
Intact seed	Uneaten seed	Intact seed	Uneaten seed	Ingested seed	Insect frass		
4.899	0.808	3891.9	641.9	3250.0	1035.4	2214.6	68.1
4.425	0.263	3768.9	224.0	3544.9	978.0	2566.9	72.4
5.999	0.411	4051.9	277.6	3774.3	1466.8	2307.5	61.1
4.766	1.495	3738.5	1172.7	2565.8	1029.7	1536.1	59.9
7.624	1.977	4571.3	1185.4	3385.9	1477.7	1908.2	56.4
6.069	0.816	6184.3	831.5	5352.8	2358.4	2994.4	55.9
4.517	1.320	3436.6	992.4	2444.2	1127.2	1317.0	53.9
4.822	1.654	2807.8	963.1	1844.7	1091.5	753.2	40.8
7.240	0.829	5327.4	610.0	4717.4	2152.9	2564.5	54.4